Mutational Analysis Provides Molecular Insight into the Carbohydrate-Binding Region of Calreticulin: Pivotal Roles of Tyrosine-109 and Aspartate-135 in Carbohydrate Recognition†

Mili Kapoor,‡,¶ Lars Ellgaard,§,¶ Jayashree Gopalakrishnapai,‡ Christiane Schirra,§ Emiliano Gemma,# Stefan Oscarson,# Ari Helenius,§ and Avadhesha Surolia*,‡

Molecular Biophysics Unit, Indian Institute of Science, Bangalore 560 012, India, Institute of Biochemistry, ETH-Zurich, Hoenggerberg, CH − 8093, Switzerland, and Department of Organic Chemistry, Arrhenius Laboratory, Stockholm University, S-106 91 Stockholm, Sweden

Received August 26, 2003; Revised Manuscript Received October 30, 2003

ABSTRACT: Calreticulin (CRT) is a lectin chaperone present in the lumen of the endoplasmic reticulum. It interacts with various glycoproteins by binding via their attached $Glc_1Man_9GlcNAc_2$ moiety. To provide further insight into these lectin−glycan interactions, we are investigating the interaction of CRT with various sugars. We have earlier modeled the complex between CRT and the Glc_1Man_3 tetrasaccharide, a derivative of the native $Glc_1Man_9GlcNAc_2$ sugar moiety. Here, we have systematically mutated the residues implicated by the model in the interaction of CRT to its sugar substrates and categorized the role played by each of the subsites of calreticulin toward the glycan binding. The CRT mutants Y109F and D135L did not show any binding to the sugar substrates interacting with the wild-type protein, demonstrating the great importance of these residues in the carbohydrate-binding site of CRT. Also, D317L and M131A showed weak affinity toward the trisaccharide. The mutation of residues from the primary binding site of CRT, i.e., those interacting with glucose, appears to be far less tolerated as compared to mutations in residues that interact with the mannose residues of the glycan. Also, methyl-2-deoxy-glucopyranosyl-α(1→3)-mannopyranoside failed to bind, asserting to the significance of the interactions between the primary binding site of CRT and the 2′-OH of the glucose residue of the oligosaccharide substrate in generating specificity for this recognition. These studies provide detailed molecular insight into the sugar binding specificity of CRT.

Several intracellular lectins such as calreticulin (CRT),[1] calnexin (CNX), endoplasmic reticulum (ER)-Golgi intermediate compartment (ERGIC)-53, and vesicular integral membrane protein (VIP)-36 play a role in the secretory pathway as chaperones and sorting receptors for a great number of glycoproteins. Interactions mediated by these lectins have important implications in the correct folding and trafficking of many cellular proteins (*1*, *2*).

CRT and CNX are molecular chaperones present in the ER, and segments of these proteins share a high degree of amino acid identity ranging from 42 to 78% (*3*). While CNX is a type-I integral membrane protein, CRT is a soluble protein. Whereas classical chaperones associate with the peptide moiety of their substrates, CRT and CNX bind their glycoprotein substrates primarily via monoglucosylated glycans ($Glc_1Man_{7-9}GlcNAc_2$), which occur as partially trimmed intermediates of the original core glycan ($Glc_3Man_9GlcNAc_2$). Soon after transfer to the nascent polypeptide chain, the successive action of glucosidase I and II leads to the cleavage of two terminal glucose molecules on the core glycan, and thereby to the formation of the monoglucosylated glycoprotein. This form of the glycoprotein is a substrate for CRT and CNX (*4*−*8*). In addition to these two chaperones, other proteins such as the thiol-disulfide oxidoreductases ERp57 and PDI assist the folding of glycoproteins in the ER. Indeed, enhanced redox activity of ERp57 has been observed in vitro upon association with CRT and CNX (*9*). Cleavage of the terminal glucose moiety by glucosidase II prevents the interaction of the glycoprotein with CRT and CNX. If the glycoprotein is not correctly folded, it is recognized by the UDP-glucose:glycoprotein glucosyl transferase. This enzyme acts as a folding sensor and reglucosylates the non-native glycoproteins to promote their renewed association with CRT and CNX (*10*, *11*). In this way, the cycle of deglucosylation and reglucosylation of glycoproteins facilitates their correct folding. In addition to the glycan-based contacts with substrate proteins, there is also evidence that CRT and CNX can interact with substrates through protein−protein contacts (*12*−*14*). Thus, both these lectin

† This investigation was supported by grants from the Department of Science and Technology, Government of India (to A.S.), and partially from the Swiss National Research Foundation and the ETH Zurich to L.E.

* Corresponding author: Prof. A. Surolia, Molecular Biophysics Unit, Indian Institute of Science, Bangalore 560012, India. Tel: 91−80−2932714, Fax: 91−80−3600535, E-mail: surolia@mbu.iisc.ernet.in.

‡ Indian Institute of Science

§ ETH-Zurich.

Stockholm University.

¶ Joint first coauthors.

[1] Abbreviations: CRT, calreticulin; CNX, calnexin; ER, endoplasmic reticulum; ITC, isothermal titration calorimetry.

10.1021/bi0355286 CCC: $27.50
Published on Web 12/10/2003

Table 1: Overview of Oligonucleotide Primers Used to Generate the CRT Mutants

oligo	sequence (5′-3′)
CRTY109Fforward	GACTGTGGGGGCGGGTTCGTGAAGCTGTTTCC
CRTY109Freverse	GGAAACAGCTTCACGAAGCCGCCCCCACAGTC
CRTD135Lforward	CATCATGTTTGGTCCGCTCATCTGCGGTCCTGGC
CRTD135Lreverse	GCCAGGACCGCAGATGAGCGGACCAAACATGATG
CRTD125Lforward	CCAGAAGGACATGCATGGACTCTCAGAATATAACATCATGTTTGG
CRTD125Lreverse	CCAAACATGATGTTATATTCTGAGAGTCCATGCATGTCCTTCTGG
CRTD125Kforward	CCAGAAGGACATGCATGGAAAGTCAGAATATAACATCATGTTTGG
CRTD125Kreverse	CCAAACATGATGGTATATTCTGAGGCTCCATGCATGTCCTTCTGG
CRTD125Gforward	CCAGAAGGACATGCATGGAGGCTCAGAATATAACATCATGTTTGG
CRTD125Greverse	CCAAACATGATGTTATATTCTGAGGCTCCATGCATGTCCTTCTGG
CRTY128Fforward	GCATGGAGACTCAGAATTTAACATCATGTTTGGTCCGG
CRTY128Freverse	CCGGACCAAACATGATGTTAAATTCTGAGTCTCCATGC
CRTD317Lforward	GCTGTACTGGGCTTACTCCTCTGGCAGGTCAAGTCTGGC
CRTD317Lreverse	GCCAGACTTGACCTGCCAGAGGAGTAAGCCCAGTACAGC
CRTR73Lforward	GACAAGCCAAGATGCCCTGTTTTACGCGCTGTCCGCC
CRTR73Lreverse	GGCGGACAGCGCGTAAAACAGGGCATCTTGGCTTGTC
CRTM131Aforward	CTCAGAATATAACATCGCGTTTGGTCCGGACATCTGC
CRTM131Areverse	GCAGATGTCCGGACCAAACGCGATGTTATATTCTGAG
PdomFor	TTGGATCCAAGAAGATTAAGGATCCTGACGC
PGex3′	CCGGGAGCTGCATGTGTCAGAGG
CRTFor	CCGAAGATCTGACCCTGCCATCTATTTCAAAGAG
CRTSSforward	CCGGATCCGACCCTGCCATCTATTTCAAAGAG
CRTPdomreverse	ATGAATTCCTAGTCTAAGCCCAGTACAGC

chaperones may play an additional role in protein folding similar to that of more classical chaperones.

The structure of the lumenal domain of CNX was reported recently (*15*). It consists of a globular lectin domain and a long hairpin loop, known as the P-domain. The NMR structure of the CRT P-domain shows a structure highly similar to the CNX P-domain (*16*). The binding site for the terminal glucose moiety of the carbohydrate is located in the lectin domain, whereas the P-domain provides a binding-site for the associated co-chaperone ERp57 (*17*, *18*). Molecular modeling of the CRT lectin domain based on the CNX structure, followed by modeling of the interaction between the glucosylated arm of the high-mannose oligosaccharide using the bound glucose as an anchor, indicated several potential hydrogen bonds between the sugar residues and CRT side chains (*19*). The thermodynamic analysis of the interaction of CRT to the tetrasaccharide substrate (Glcα1-3Manα1-2Manα1-2ManαMe) revealed information about the nature and the relative contribution of various noncovalent forces in determining this recognition.

In this paper, we report the generation of mutants of the CRT carbohydrate-binding site that were implicated to play an important role in the recognition of the oligosaccharide ligand, their overexpression, purification, and characterization. Isothermal titration calorimetry was used to quantitatively determine the effect of each mutation on the binding of sugars to CRT. The studies reported here reveal that Tyr-109, Met-131, Asp-135, and Asp-317 play pivotal roles in the binding of the oligosaccharide to CRT.

EXPERIMENTAL PROCEDURES

Materials. Media components were obtained from Himedia (Delhi, India). GST-agarose, reduced glutathione, thrombin, IPTG, MOPS, and SDS−PAGE reagents were obtained from Sigma Chemicals Co. (St. Louis, MO).

Construction of Y109F, D135L, D125L, D125G, D125K, and Y128F CRT Mutants. The single point mutations of Tyr109 to Phe (Y109F), Asp135 to Leu (D135L), Asp125 to Leu (D125L), Asp125 to Gly (D125G), Asp125 to Lys (D125K), and Tyr128 to Phe (Y128F) of rat CRT were generated using the Quick Change kit (Stratagene, La Jolla, CA). The primers used in the mutagenic PCR reactions are listed in Table 1. A pRSET A-derived vector (*20*) containing residues 1−337 of rat CRT (GenBank accession number X79327) was used as the template plasmid for all the reactions. To allow for subsequent cloning steps to be performed using the BamHI site immediately preceding the first codon of the CRT sequence, the internal BamHI site within the CRT gene was mutated by introducing a T → C base pair change at position 643. This base pair change introduces a silent mutation in the codon for Asp-193. For all the mutants, restriction digestion with BamHI and KpnI releases a 816-bp fragment encompassing the site of mutation. These fragments were cloned into the pGEX-KG/CRTwt vector (*21*), thus generating expression plasmids containing the full-length sequences of rat CRT harboring the wanted mutations in frame with an N-terminal GST-tag.

Construction of D317L, D125L/D135L, Y109F/D125L/D135L, R73L, and M131A CRT Mutants. The Asp317 to Leu (D317L) mutant was generated by PCR overlap extension using the pGEX-KG/CRTwt as template. The two PCR products with overlapping ends were generated by using the "PdomFor" primer together with "CRTD317Lrev" and "CRTD317Lfor" together with "PGex3′". The combined PCR product was digested with KpnI and EcoRI and cloned into pGEX-KG/CRTwt digested with the same two enzymes. The double mutant (D125L/D135L) was generated by PCR overlap extension (*22*) using the pGEX-KG/CRTD125L as template. The two PCR products with overlapping ends were generated by using the "CRTSSforward" primer together with "CRTD135Lreverse" and "CRTD135Lforward" together with "CRTPdomreverse". The combined PCR product was digested with BamHI and KpnI and cloned into pGEX-KG/CRTwt. Subsequently, the triple mutant Y109F/D125L/D135L was generated by taking advantage of a NspI restriction site positioned between the codons for Y109 and D125. Thus, the BamHI−NspI fragment comprising the Y109F mutation and the NspI−KpnI fragment containing

the D125L/D135L double mutation were ligated into BamHI−KpnI digested pGEX-KG/CRTwt in a three-point ligation.

Arg73 to Leu (R73L) and Met131 to Ala (M131A) mutants were generated by PCR overlap extension using pGEX-KG/CRTwt as the template. In the case of the R73L mutation, the two PCR products with overlapping ends were generated by using "CRTFor" primer together with "CRTR73Lreverse" and "CRTR73Lforward" together with "PGex3′". The combined PCR product was digested with BglII and EcoRI and cloned into BamHI and EcoRI digested pGEX-KG/CRTwt. M131A was constructed in similar fashion by using "CRTM131Aforward" and "CRTM131Areverse" primers. The correct sequences of all constructs were verified by DNA sequencing.

Expression and Purification of Recombinant CRT. The GST-CRT wild-type and mutant fusion proteins were purified as described earlier (*19*, *21*). To remove the GST-tag from CRT, the GST−CRT protein in 50 mM Tris-Cl (pH 7.4) containing 150 mM NaCl and 10 mM $CaCl_2$ was incubated with thrombin (NIH units: 74 units/mg of protein) at 25 °C for 12 h. The reaction was stopped by the addition of PMSF and the mixture was loaded onto a 20-mL glutathione-agarose affinity column at 4 °C. The mixture was allowed to interact with the matrix for 1 h, and the flow-through was collected as 0.5-mL fractions at a flow rate of 15 mL/h. The fractions were checked for cleavage on a 10% SDS−PAGE. The fractions containing pure CRT were pooled and concentrated using 10-kDa centripreps (Amicon) for further experiments. The molecular weight of purified wild-type and mutant CRTs was further confirmed on a Ultraflex TOF/TOF MALDI mass spectrometer (Bruker Daltonik).

Immunodetection of Recombinant CRT. The protein bands run on 10% SDS−PAGE were transferred onto PVDF membranes (Immobilon, Millipore) using Pharmacia LKB mutiphor II semi-dry Western blot apparatus. The presence of CRT was detected using rabbit anti-CRT antibody (Affinity BioReagents Inc., Golden, CO) as the primary antibody and goat anti-rabbit antibody conjugated to HRP (Bangalore Genei, Bangalore, India) as the secondary antibody. The anti-CRT antibody is a polyclonal antibody raised against recombinant full-length CRT. The gel was also probed using anti-GST antibody conjugated to HRP (Bangalore Genei). Both the blots were developed using 3-amino-9-ethylcarbazole (AEC) and hydrogen peroxide.

Protein Estimation. E_{280} of wild-type and mutant CRT was estimated using the ProtParam tool at http://tw.expasy.org/tools/protparam.html.

Gel Filtration Analyses. Purified CRT (2 mg/mL) was injected onto a Superdex200 HR10 × 300 mm column (Amersham Biosciences) equilibrated in 20 mM Tris-Cl, 150 mM NaCl (pH 7.4), containing 5 mM $CaCl_2$, connected to an ÄKTA design system at room temperature. The column flow rate was maintained at 0.3 mL/min. The column was calibrated using standards of known molecular weight.

Circular Dichroism Studies. CD spectra were recorded on a Jasco J-715 spectropolarimeter at 20 °C. CRT (6 μM) in 10 mM MOPS, 5 mM $CaCl_2$, and 150 mM NaCl (pH 7.4) was used during the measurements. Far-UV CD spectra were recorded from 200 to 250 nm at 0.5-nm intervals with a spectral bandwidth of 2 nm using a 1-mm cuvette. The program, K2D, available at http://www.embl-heidelberg.de/~andrade/k2d.html, was used to estimate the percentages of protein secondary structure from the CD spectra (*23*). Near-UV CD spectra were recorded from 250 to 350 nm using a 10-mm cuvette. Each scan represents an average of six scans.

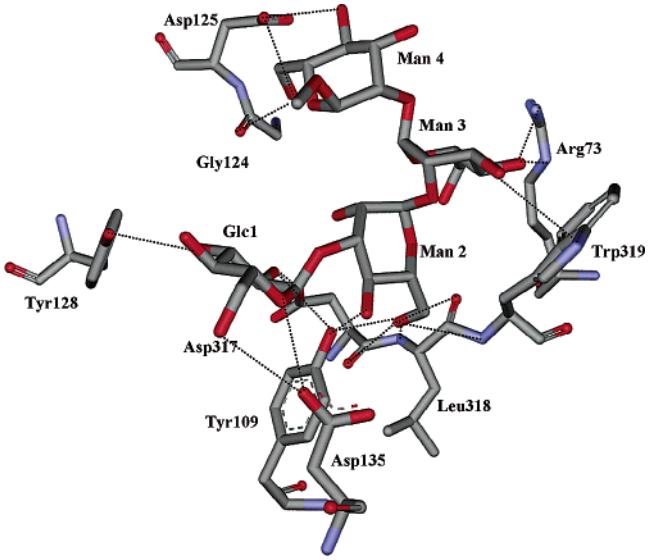

FIGURE 1: A schematic representation obtained from our previous modeling studies (*19*) of the interaction of tetrasaccharide (Glcα1-3Manα1-2Manα1-2ManαMe) with the active site residues. The amino acid residues and the tetrasaccharide are shown in elemental colors. Hydrogen bonds within a distance of 2.5−3.35 Å are denoted by dotted lines. The sugar residues have been numbered from the nonreducing end.

Synthesis of Sugars. Glucosylated oligosaccharides were synthesized chemically and were available from a previous study (*19*). Carbohydrate concentrations were determined by a modification of the phenol-sulfuric acid method of Dubois et al. (*24*, *25*). Synthesis of the methyl-2-deoxy-glucopyranosyl-α(1→3)-mannopyranoside was carried out as described in ref *26*.

Isothermal Titration Calorimetry. ITC was performed using VP−ITC calorimeter from Microcal Inc. (Northampton, MA) as described previously by Wiseman et al. (*27*). 90 μM protein (in 10 mM MOPS, 5 mM $CaCl_2$, 150 mM NaCl, pH 7.4) in sample cell, volume 1.4181 mL, was titrated with 10 times excess sugar (present in same buffer) from a 300 μL stirrer syringe. The titrations were performed while samples were being stirred at 400 rpm at the required temperatures. An interval of 3 min between each injection was given for baseline to stabilize. The heats of dilution of the sugar were subtracted from the titration data. The data so obtained were fitted via nonlinear least squares minimization method to determine binding stoichiometry (n), the binding constant (K_b), and the change in enthalpy of binding (ΔH_b°) using Origin software (Microcal) as described in ref *28*. The change in free energy of binding (ΔG_b°) is calculated from eq 1:

$$\Delta G_b^\circ = -RT \ln K_b \qquad (1)$$

where R is the gas constant and T is the temperature in Kelvin. The thermodynamic quantities were used to determine the change in entropy (ΔS) from eq 2:

$$\Delta G_b^\circ = \Delta H_b^\circ - T\Delta S \qquad (2)$$

The experimental conditions ensured that c value ranged from

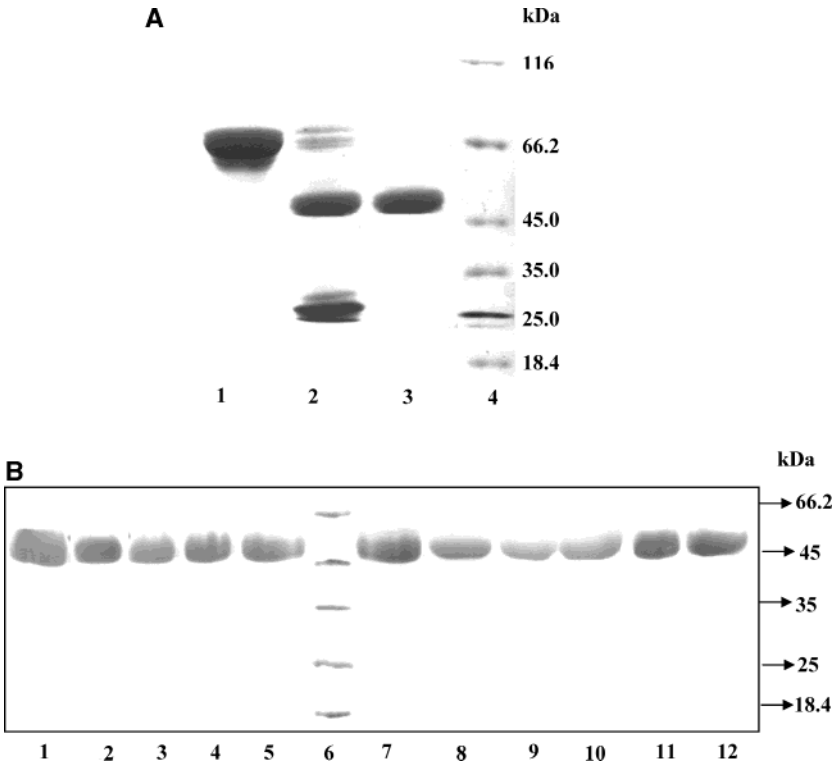

FIGURE 2: Cleavage of GST−CRT by thrombin to obtain CRT. 10% SDS−PAGE showing the cleavage of GST−CRT (in 50 mM Tris-Cl, pH 7.4, containing 150 mM NaCl and 10 mM $CaCl_2$) by thrombin (74 NIH units/mg of protein) at 25 °C for 12 h. CRT was further purified by collecting flow-through from a glutathione-agarose affinity column. Lane 1: GST-CRT; lane 2: thrombin cleaved GST-CRT; lane 3: Pure CRT; lane 4: MBI molecular weight markers. (B) SDS−PAGE analysis of mutants. The fusion protein of various mutants was cleaved with thrombin, purified as described above, and run on 12% SDS−PAGE (lanes 1−5: Y109F, D135L, D317L, Y128F, D125L; lane 6: MBI molecular weight markers; lanes 7−12 M131A, R73L, D125G, D125K, D125L/D135L, D125L/D135L/Y109F). All the mutants run at the same position as the wild-type CRT.

2 to 130, where $c = K_b M_t(0)$, and $M_t(0)$ is the initial macromolecule concentration for all the titrations. The value of the binding constant (K_b) was used to compare the relative binding of the various CRT mutants with the saccharides.

RESULTS

In our previous study, molecular modeling implicated certain residues of CRT in the binding to its carbohydrate substrate (Figure 1) (*19*). We also studied the thermodynamics of the interaction of CRT with various saccharides that were truncated versions of the glucosylated arm of $Glc_1Man_{7-9}GlcNAc_2$. On the basis of this, we could derive the contributions made by each of the subsites of the CRT sugar-binding site. As shown in Figure 1, these residues are expected to make several key hydrogen bonding interactions especially with the nonreducing end glucose of the oligosaccharide. Here, we have examined the effect of mutations that span the tetrasaccharide (Glcα1-3Manα1-2Manα1-2ManαMe)-binding region, on the carbohydrate recognition by CRT.

Purification of CRT. As shown in Figure 2, CRT was initially purified as a fusion protein to glutathione-*S*-transferse (GST) on a glutathione-agarose column. In our previous study, we analyzed the interaction between the various saccharides and the GST−CRT fusion protein by ITC (*19*). To rule out any nonspecific contribution from the presence of GST, we decided to use CRT devoid of GST for the studies presented here. The cleavage of GST−CRT by thrombin led to the appearance of two bands on SDS−PAGE of 50 (±5) and 26 (±1.5) kDa corresponding to CRT and GST, respectively (Figure 2A). Pure CRT was separated from this mixture by reloading it on the glutathione-agarose column and collecting the flow-through. Mutants of CRT were also cleaved and purified in a similar manner, and the mobility as analyzed by SDS−PAGE was similar to the wild-type CRT (Figure 2B). The expected molecular mass of CRT as calculated using the ProtParam tool at http://kr.expasy.org/tools/ was M_r 46378.3. The molecular weight of purified CRT was further confirmed by MALDI mass spectrometry to M_r 46368.3 (±2) Da, which rules out the possibility of our working with truncated versions of CRT. The molecular weights of the mutant CRTs were also confirmed by MALDI and were found to be of the expected molecular masses.

Immunodetection of CRT. The expression of recombinant CRT was confirmed using anti-CRT and anti-GST antibodies. As shown in Figure 3A, anti-CRT antibody detected GST−CRT fusion protein (lane 1), thrombin-cleaved GST−CRT (lane 2) and purified CRT (lane 3). Anti-GST antibody also confirmed the cleavage of GST from GST−CRT as seen from the appearance of a 26-kDa band after thrombin cleavage of GST−CRT (Figure 3B). The purified mutants could also be detected by anti-CRT antibody (Figure 3C).

Gel Filtration Analyses. Changes in the overall shape or the quaternary structure of the molecule potentially introduced by mutagenesis was first probed using size exclusion chromatography. Native CRT eluted as a single peak at a volume of 12.4 mL on a Superdex-200 gel-filtration column (Figure 4). This elution volume corresponds to a significantly larger protein than expected for CRT. We also analyzed the elution behavior of the various mutants. Importantly, all the mutants eluted at the same position in gel filtration experi-

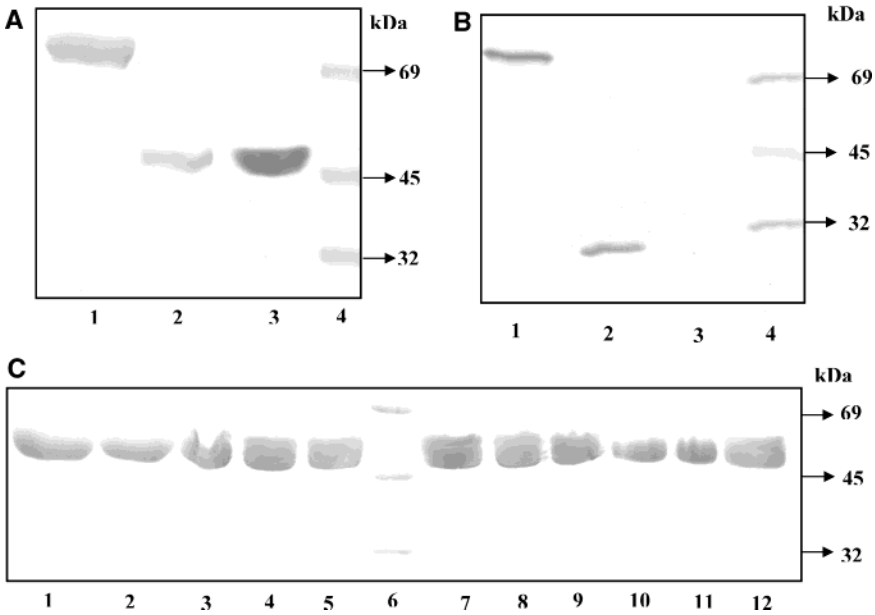

FIGURE 3: Western blot analysis of recombinant wild-type CRT using anti-CRT (A) and anti-GST (B) antibodies. Duplicate protein samples were run on 10% SDS−PAGE and transferred onto PVDF membranes. The blot was developed using anti-CRT (A) and anti-GST (B) antibodies. Lane 1: recombinant GST-CRT; lane 2: recombinant GST-CRT cleaved with thrombin; lane 3: purified CRT; lane 4: Prestained protein molecular weight markers. (C) Western blot analysis of mutants using anti-CRT antibody. Purified mutant protein obtained after cleavage of the fusion proteins were analyzed by Western blot using anti-CRT antibody (lanes 1−5: Y109F, D135L, D125L, D317L, and Y128F; lane 6: Prestained protein molecular weight marker; lanes 7−12: M131A, R73L, D125G, D125K, D125L/D135L, D125L/D135L/Y109F).

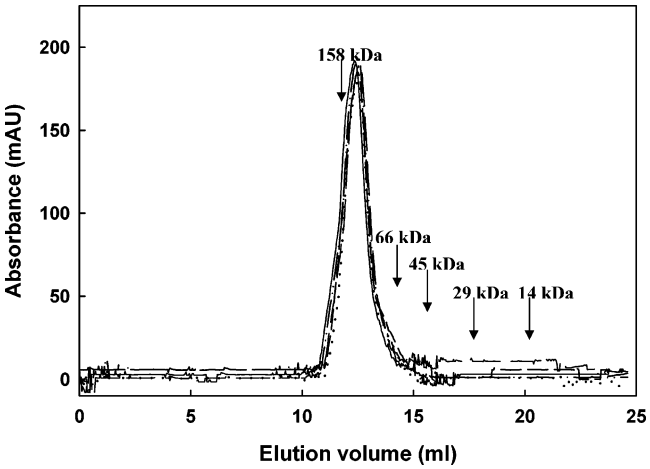

FIGURE 4: Gel filtration profile of wild-type and mutant CRT. Gel filtration profile of the wild-type (short dash), Y109F (line), M131A (long dash), D135L (dotted), and D317L (dash−dot−dot) mutants. CRT elutes as a single peak at an elution volume of 12.4 mL on a Superdex-200 gel filtration column. Arrows show the elution volume of the standard molecular weight markers. The standards used were 1, lysozyme (14 kDa); 2, carbonic anhydrase (29 kDa); 3, ovalbumin (45 kDa); 4, bovine serum albumin; (66 kDa); 5, aldolase (158 kDa).

ments, indicating that the mutations did not alter the overall shape or the quaternary structure of CRT.

Circular Dichroism Analyses. To investigate potential perturbations in the secondary and tertiary structure of CRT mutants, we used CD spectroscopy. The CD spectra of the mutant CRT variants were similar to the spectrum obtained for the wild-type CRT (Figure 5A), i.e., the data showed that there were no changes in the molar ellipticity in the secondary structural region between the various mutant and native CRT. Moreover, the overall shape of the spectra remained the same. The calculated values of the secondary structures based on the CD spectra for the wild-type CRT are α-helix = 8.0% (±2), *β*-sheet = 44% (±6), and random coil = 48% (±4.5). The calculated secondary structures for the mutants were the same as the wild-type. This indicated that the various amino acid substitutions had no effect on the overall folding of the resultant mutant protein.

In the near-UV spectra, there were slight differences in the molar ellipticities of the wild type, the Y109F and the Y128F mutants (Figure 5B). Thus, there is an appearance of a minor hump at 256 nm in the spectra obtained for Y109F and Y128F mutants as well as a reduction in intensity at 270−295 nm. These minor differences in the absorption can be attributed to the changes of the chromophoric amino acids, namely, the replacement of tyrosine (absorption maximum at 278−280 nm) with phenylalanine (absorption maximum at 254−256 nm). M131A, D135L and D317L gave tertiary CD spectra similar to the wild-type protein.

Isothermal Titration Calorimetry. First, we characterized the thermodynamics of sugar interaction by the CRT used here and the GST−CRT used in our previous study, to ascertain that these proteins behaved similarly. As can be seen from Table 2, we observed no differences in the thermodynamic parameters obtained for CRT and GST-CRT (the values for the latter reported in the previous study; *19*). Table 3 shows the contribution in ΔG made by each of the subsites obtained by comparing the ΔG values of a pair of saccharides using glucose as a reference compound. Although the monosaccharide per se shows binding to CRT and the disaccharide even better, for comparing the binding interactions of the various mutants we have used the trisaccharide and the tetrasaccharide as the errors associated with the various thermodynamic parameters determined were lower in the case of tri- and tetrasaccharide as compared to the mono- and disaccharide.

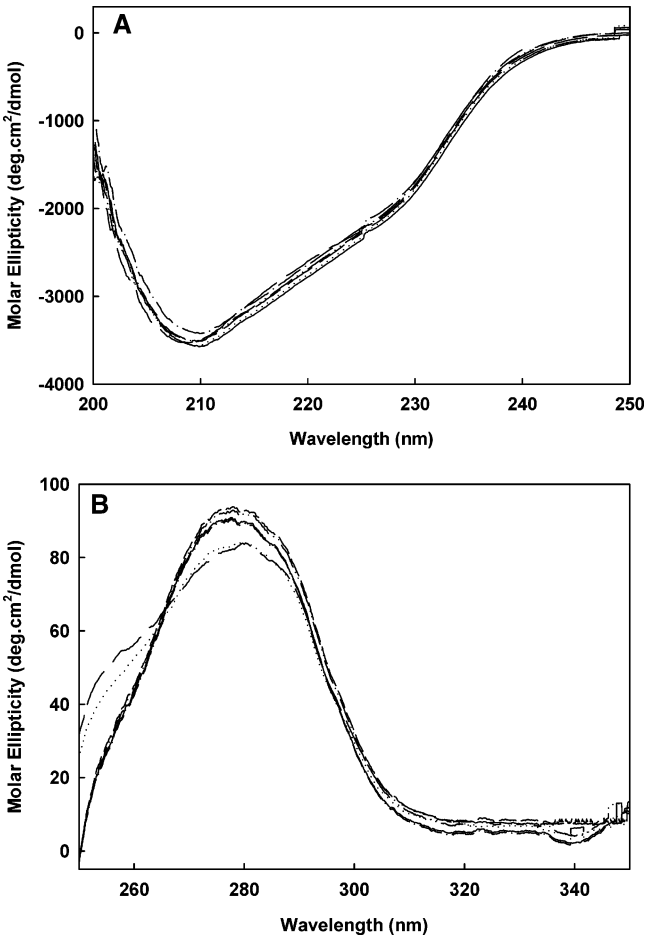

FIGURE 5: CD spectrum analysis of wild-type, Y109F, Y128F, M131A, D135L, and D317L CRT. (A) Far-UV spectra obtained for 6 μM protein in 10 mM MOPS, 150 mM NaCl pH 7.4 containing 5 mM $CaCl_2$ at 20 °C from 200 to 250 nm using the 1-mm cuvette. (B) Near-UV spectra obtained for 6 μM protein in the same buffer from 230 to 350 nm at 20 °C using the 10-mm cuvette. Wild-type (short dash), Y109F (long dash), Y128F (dotted), M131A (dash−dot), D135L (dash−dot−dot), and D317L (line).

To characterize the importance of the glucose-binding region of CRT, we made the following CRT mutants: Y109F, Y128F, M131A, D135L, and D317L. In addition, we also created the double mutant D125L/D135L and the triple mutant Y109F/D125L/D135L. Although the substitution of Asp with Leu is not as conservative as substitutions with Asn or Ser would have been, this choice is still warranted in this study, as we wanted to disrupt the hydrogen bonding potential of the Asp residue. A CRT mutant with the replacement of Asp to Ser or Asn would still potentially hydrogen bond with the sugar. Furthermore, as tested in our model, the intended mutations did not lead to any steric hindrance. Hence, we mutated Asp to Leu. Of all the residues studied, Tyr-128, Asp-135, Met-131, and Asp-317 are predicted to interact exclusively with the glucose moiety (see Figure 1). However, in addition to having predicted hydrogen-bonding interactions with glucose, Tyr-109 also interacts with the first mannose from the nonreducing end (Man2). Other than the interactions with Tyr-109, Man2 is predicted to interact only with the main chain N and O atoms of Asp-317, Leu-318, and Trp-319. To characterize the contribution made by Man3 to the CRT−glycan interaction, we made the R73L CRT mutant and to probe the interaction of Man4 with CRT, we initially made only the D125L CRT mutant. The numbering of the residues mentioned in the manuscript refers to the full-length CRT sequence including the signal sequence.

Hydrogen Bonding Interactions between O2H of Glucose and CRT. In the model (Figure 1), Tyr-109 makes three hydrogen bonds with the tetrasaccharide (Glcα1-3Manα1-2Manα1-2ManαMe), one with the glucose and two with the first mannose from the nonreducing end. On the basis of our model, the hydroxyl group of Tyr-109 should make polar (hydrogen bonding) interactions with the equatorially oriented hydroxyl group at the C2 position of glucose as well as interactions with the O4H and O6H of the first mannose from the nonreducing end. In accordance with these predictions, the Y109F mutant did not show any binding to any of the complementary ligands including the trisaccharide. A similar result was obtained for Asp-317, where the OD2 makes hydrogen-bonding interactions with O2H of the glucose moiety. The mutation of Asp-317 to Leu led to a loss of binding activity (≥99%), further demonstrating the importance of the interaction between the 2′-OH of glucose and CRT.

The only difference between glucose and mannose is related to the orientation of the hydroxyl group at their C2 position, whereas it is equatorial in the former, it is axial in the latter monosaccharide. Hence, to probe the role of hydrogen bonding between OH at C2 of glucose and the hydroxyl groups of Tyr-109 and Asp-317 further, a complementary approach to the site-specific mutagenesis involving a modified carbohydrate ligand was used. Replacement of the hydroxyl group of monosaccharide ligand(s) with a deoxy group provides further evidence for the indispensability of the key hydrogen bonding interactions between the sugar occupying the primary site and the corresponding loci in the combining site of the lectin (*29*). We, therefore, studied the binding of wild-type CRT to the disaccharide, methyl-2-deoxy-glucopyranosyl-α(1→3)-mannopyranoside. The 2-deoxy derivative of the disaccharide did not show any binding to wild-type CRT, further attesting to the importance of hydrogen bonding interactions between the equatorially oriented hydroxyl at C2 of glucose and the protein (Figure 6A). This is also consistent with our earlier observation that Manα1-3Man does not bind to CRT (*19*). These studies thus underscore that while glucose by itself is an extremely poor ligand, it is indispensable for recognition by CRT by virtue of its involvement in key hydrogen bonds with the chaperone where it occupies the primary binding site.

Hydrogen Bonding Interactions between Hydroxyl Groups Other than the 2′-OH of Glucose and CRT. Having established the importance of 2′-OH of the glucose moiety for the interaction with CRT, we next investigated the role of hydrogen bonding interactions between hydroxyl groups other than 2′-OH and CRT. Asp-135 was predicted to make two hydrogen bonds with the tetrasaccharide. The OD2 atom of Asp-135 hydrogen bonds to O10 and O6H of glucose (Figure 1). Similar to the effects observed for the Y109F mutant, the mutation of Asp-135 to leucine led to a total loss in binding of trisaccharide to CRT (Table 2). Also, the double (D125L/D135L) and triple (Y109F/D125L/D135L) mutants were inactive (Table 2).

Tyr-128 is predicted to make a hydrogen bond via its hydroxyl moiety with O3H of glucose. The mutation of Tyr to Phe decreases the binding affinity by 80%, with the

Table 2: Thermodynamic Quantities for the Binding of Wild-Type and Mutant CRT to Saccharides at 293 K[a]

construct	ligand	n	$K_b \times 10^{-4}$ (M^{-1})	$-\Delta G_b^\circ$ (kcal/mol)	$-\Delta H_b^\circ$ (kcal/mol)	ΔS_b (cal mol^{-1} K^{-1})
wild-type	glucose	1.05 (±0.12)[b]	0.006(±0.001)	2.36(±0.12)	0.15(±0.11)	7.51(±0.91)
wild-type	disaccharide	0.91(±0.03)	1.99(±0.09)	5.75(±0.07)	2.05(±0.13)	12.66(±0.11)
wild-type	trisaccharide	0.88(±0.03)	58.8(±2.1)	7.71(±0.05)	7.22(±0.063)	1.57(±0.11)
wild-type	tetrasaccharide	0.91(±0.05)	104(±1.8)	8.09(±0.03)	10.42(±0.12)	−8.03(±0.07)
Y109F	trisaccharide	no binding				
D135L	trisaccharide	no binding				
D317L	trisaccharide	0.87(±0.2)	0.45(±0.13)	4.88(0.35)	3.3(±0.29)	5.12(±0.19)
Y128F	trisaccharide	0.94(±0.1)	11.21(±0.12)	6.76(±0.19)	5.32(±0.21)	4.91(±0.09)
M131A	trisaccharide	0.81(±0.4)	0.89(±0.21)	5.28(±0.42)	3.42(±0.3)	6.23(±0.29)
R73L	trisaccharide	0.91(±0.12)	14.82(±0.14)	6.93(±0.12)	5.92(±0.22)	3.41(±0.03)
D125L[c]	trisaccharide	0.91(±0.12)	55.91(±2.4)	7.65(±0.14)	7.35(±0.13)	1.02(±0.12)
D125L	tetrasaccharide	0.94(±0.13)	106(±2.3)	8.07(±0.03)	10.45(±0.14)	−8.13(±0.03)
D125G	trisaccharide	0.92(±0.11)	53.21(±1.91)	7.68(±0.02)	7.41(±0.09)	0.95(±0.04)
D125G	tetrasaccharide	0.89(±0.09)	103(±2.0)	8.03(±0.04)	10.38(±0.1)	−8.02(±0.12)
D125K	trisaccharide	0.95(±0.08)	56.45(±1.5)	7.71(±0.02)	7.31(±0.15)	1.36(±0.2)
D125K	tetrasaccharide	0.92(±0.05)	105(±1.9)	8.11(±0.1)	10.45(±0.09)	−8.01(±0.09)
D125L/D135L	trisaccharide	no binding				
D125L/D135L/Y109F	trisaccharide	no binding				

[a] Each value is an average of three-four determinations. [b] The values in parentheses are the standard deviations. The thermodynamic parameters for the binding of saccharides to CRT are similar to those obtained for GST-CRT(19). [c] For D125L, D125G, and D125K CRT mutants, thermodynamic parameters are shown for both the trisaccharide and tetrasaccharide as Asp-125 was predicted to interact with the fourth sugar of the tetrasaccharide. The sugars used were disaccharide (Glcα1−3ManαMe); trisaccharide (Glcα1−3Manα1−2ManαMe); tetrasaccharide(Glcα1−3Manα1−2Manα1−2ManαMe).

Table 3: Contribution of Each Subsite of CRT toward Tetrasaccharide (Glcα1-3Manα1-2Manα1-2ManαMe) Binding[a]

A B C D	ΔG_b° (kcal/mol)	$\Delta\Delta G_b^\circ$ (kcal/mol)
Glc	−2.36	0.0
Glcα1-3*Man*αMe	−5.75	−3.39
Glcα1-3Manα1-2*Man*αMe	−7.71	−1.96
Glcα1-3Manα1-2Manα1-2*Man*αMe	−8.09	−0.38

[a] The contribution of each subsite to the association of the glycan with CRT was calculated by comparing the ΔG_b° values for a pair of saccharides that differ by a single sugar residue. It is assumed that the italicized sugar residue is bound at the subsite. The saccharides are arranged in their respective subsites with the reducing end to the right.

binding constant obtained for the interaction of the trisaccharide and Y128F being 1.12×10^5 M^{-1} (Figure 6B and Table 2). Asp-317 and Tyr-128 both make interactions exclusively with glucose. However, the mutation of Asp-317 to Leu appears to be more detrimental as compared to the mutation of Tyr-128 to Phe. Earlier, it has been observed that the hydrogen bonds between a charged atom and a hydroxyl group are stronger than those involving a neutral atom (*30*). This indeed appears also to be the case for CRT−saccharide interactions.

Hydrophobic Interactions between Sugar and CRT. In addition to hydrogen bonds, Arg-73, Tyr-109, Asp-125, and Met-131 were predicted by our model to make hydrophobic interactions with the sugar. Met-131 is not involved in any hydrogen-bonding interactions and makes only hydrophobic interactions with glucose. To investigate the role played by this interaction, we mutated Met-131 to Ala. The mutation reduced the binding constant to merely 1.5 (±0.2)% of the value observed for wild-type CRT, asserting to the crucial role of a hydrophobic interaction in tethering the glucose residue in the primary site of this chaperone.

Importance of Residues Predicted for Binding of Man3 and Man4. To characterize the importance of Man3 and Man4, we mutated Arg-73 and Asp-125 to a leucine in both cases. The Nϵ atom of Arg-73 is predicted to hydrogen bond with O4H of Man3 and mutation of this residue led to a 75% reduction in the binding affinity (Table 2). This in turn indicates that amino acid side chains involved in binding to sugars occupying subsites other than the primary one are tolerated to a certain extent.

There are two hydrogen bonds predicted between Asp-125 and Man4: one between the O4H of mannose and OD1 of Asp-125 and the other between O6H and of mannose and OD2 of Asp-125. However, the D125L mutant showed similar affinities for both the tri- and tetrasaccharide substrate as observed for the wild-type protein.

A comparison of rat CRT sequence (that has been studied in the present study) with CRT from other organisms is in order at this stage. Multiple sequence alignment of CRT from different organisms along with canine CNX, for which the crystal structure was solved (*15*), provides further support to our mutational studies. As can be observed in Figure 7, the critical residues required for the binding of sugar to CRT are conserved across species. In fact Tyr-109, Met-131, Tyr-128, and Asp-135 are identical in all the sequences shown. Arg-73 is identical in all the CRTs and replaced by a conservative substitution with a lysine in CNX. A glutamate is present in the place of Asp-317 in the case of human CRT and canine CNX. This all adds further credibility to the importance shown here for these residues in the glycan binding site of CRT. On the other hand, the residue Asp-125 is not conserved, as a lysine is present in its place in human CRT and canine CNX. This again supports the experimental observation that the mutation of Asp-125 to Leu, Gly, or Lys does not affect the binding properties of CRT (see Discussion).

DISCUSSION

Hydrogen bonds play a pivotal role in imparting specificity to protein−carbohydrate interactions in addition to contributing to the energetics of binding, although nonpolar interactions are deemed essential in determining the overall stabilization of the interaction. Thus, many of the polar

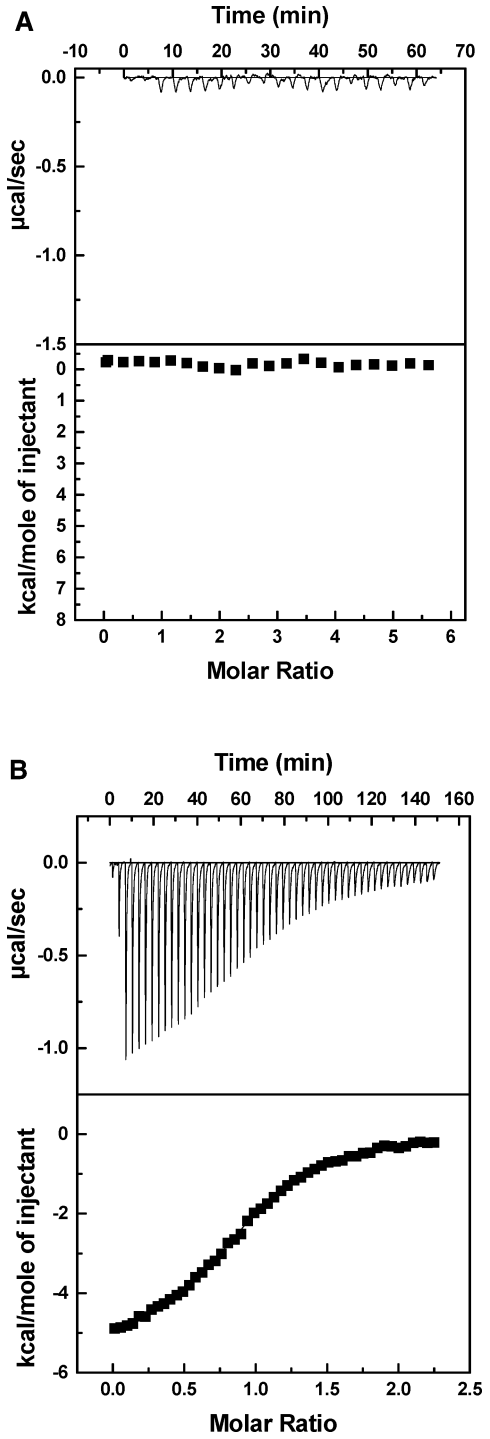

FIGURE 6: Isothermal titration calorimetry of different constructs of CRT with the saccharides. Raw data obtained after a single 2 μL preinjection followed by 6 μL injections of 1 mM sugar solution into 90 μM CRT in 10 mM MOPS buffer containing 5 mM $CaCl_2$ and 150 mM NaCl at 293 K (top). Nonlinear least-squares fit (−) of the heat released as a function of the added ligand (■) for the titration is also shown (bottom). The data were fitted to single site model. (A) Wild-type CRT and methyl-2-deoxy-glucopyranosyl-α(1 → 3)-mannopyranoside; No binding was observed. (B) Y128F CRT and trisaccharide (Glcα1-3Manα1-2ManαMe); n = 0.96 (±0.08), ΔH_b° = 5.12 (±0.11) kcal/mol and K_b = 1.18 × 10^5 (±0.15) M^{-1}. The values in brackets are the errors associated with each fitted parameter for a given experiment.

groups (hydroxyl groups and ring oxygen atoms) of the bound sugar participate in the formation of hydrogen bonds with the backbone carbonyl and amide groups as well as with the carboxyl, hydroxyl, and amide groups of amino acid side chains of the protein, while the nonpolar side chains contribute to the stability of the complex through hydrophobic interactions (*31*).

The participation of a particular amino acid residue of a protein in the interaction with a ligand can be assessed by site-directed mutagenesis. Hence, we performed a series of mutations spanning the tetrasaccharide-binding site of CRT. The expression of a recombinant GST−CRT fusion protein, the cleavage of CRT from GST−CRT and the purification of the pure CRT were confirmed using anti-CRT and anti-GST antibody. To exclude the possibility that the sugar binding of mutant CRTs was decreased due to the introduction of large structural changes, we first analyzed the oligomerization status and conformation of wild-type and mutant CRT by gel-filtration and circular dichroism (CD) spectroscopy. Thereafter, we performed a thorough analysis of the interaction of the generated CRT mutants with Glcα1-3Manα1-2ManαMe trisaccharide by ITC.

The anomalous behavior of CRT on SDS−PAGE (Figure 2) is consistent with earlier studies, which have shown that CRT migrates as a higher MW species (*32*, *33*). Also, CRT eluted at a position corresponding to 146 (±7) kDa as observed by gel-filtration chromatography (Figure 4). This is similar to the observations of Bouvier and Stafford (*33*) in which CRT eluted at a position corresponding to 158 kDa. The anomalous behavior of CRT is not surprising as the recent structural and biophysical analysis obtained for CRT and CNX demonstrated both proteins to be highly asymmetric molecules (*15*, *16*, *33*, *34*). Thus, the unusual behavior of CRT on gel filtration has been ascribed to the elongated structure of the protein in solution (*33*, *34*). Taken together, the gel filtration analysis and the CD spectroscopy studies showed no evidence of significant conformational changes in any of the CRT mutants in comparison to the wild-type protein. Although these data do not allow us to rule out more subtle conformational changes, it is likely that such changes also do not occur.

To analyze the importance of each of the subsites, we created mutations in the residues that were predicted by us to interact with each saccharide unit of the sugar. On the basis of mutagenesis studies we can conclude that Y109, M131, D135, and D317 play important roles in the sugar-binding site of CRT. From the findings described above, it is clear that Asp-135 and Tyr-109 are both likely to be involved in key polar interactions with glucose. Also, the double (D125L/D135L) and triple (Y109F/D125L/D135L) mutants involving these two residues were, as expected, demonstrated to be inactive (Table 2). The observations thus highlight that mutation of these side chains lead to the abrogation of crucial interactions with the glucose residue, which occupies the primary binding site of this chaperone. The ensuing complete loss of binding demonstrates the validity of our model. Similar to what is observed here for CRT, a number of mutations that prevent hydrogen bonding interactions between legume lectins and the complementary monosaccharide ligand that reside in the primary binding site in the corresponding lectin invariably give rise to inactive mutants (*31*).

The D125L mutant did not show any differences in the affinities toward tri- and tetrasaccharide as compared to the wild-type CRT. This finding could have two potential

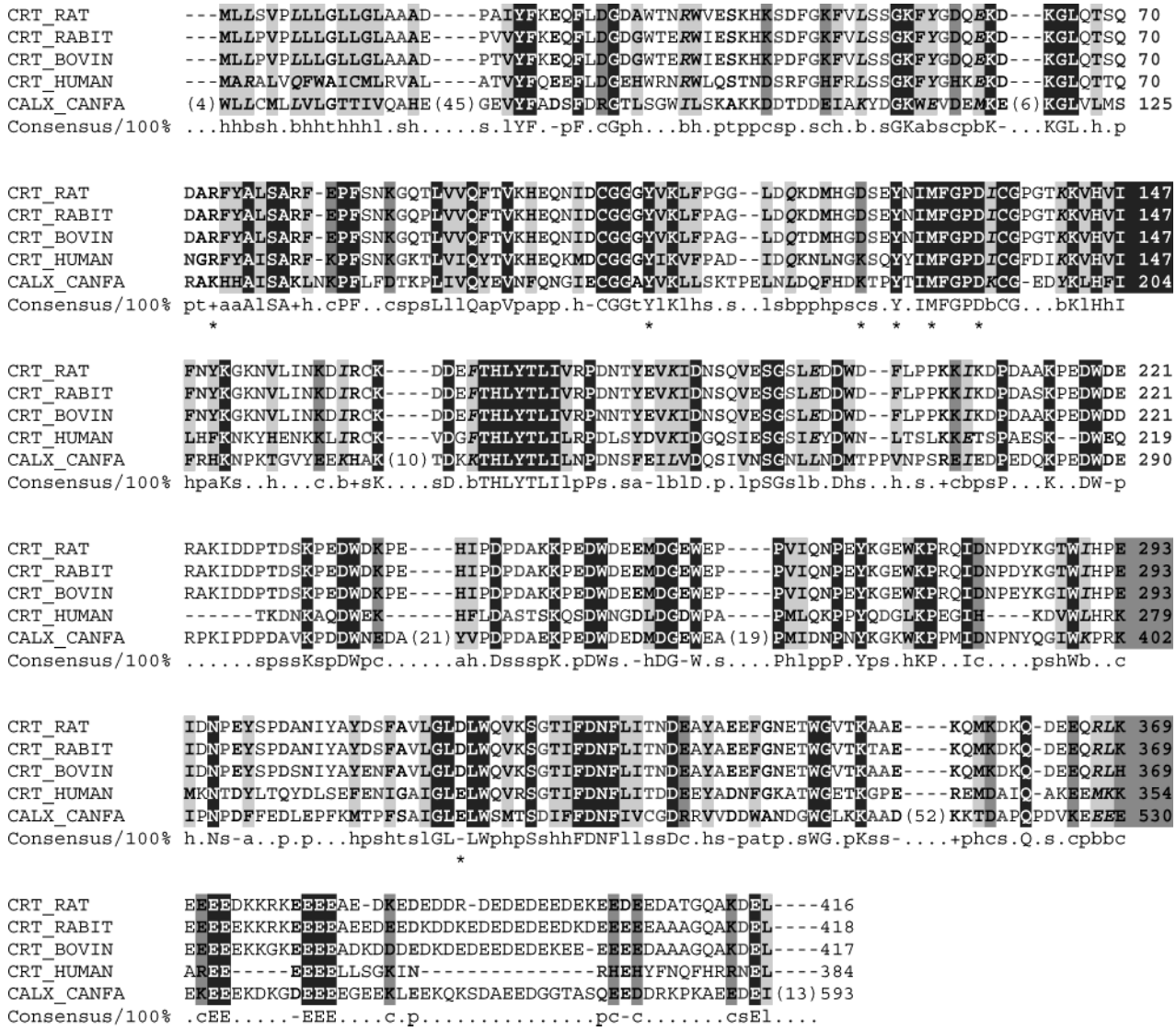

FIGURE 7: Mutiple sequence alignment of CRT from different organisms along with canine calnexin. Amino acid sequence of rat CRT (Ac. No. P18418) is compared with human CRT (Ac. No. Q96L12), rabbit CRT (Ac. No. P15253), bovine CRT (Ac. No. P52193), and canine calnexin (Ac. No. P24643). The residues mutated in the present study are indicated as asterisk (*). Color scheme: Conserved residues shown are in bold with black background, negative residues are indicated by (−), positive by (+), aliphatic by (l), aromatic by (a), tiny by (t), small by (s), big by (b), charged by (c), polar by (p), and hydrophobic by (h) (all below the alignment). The figure was generated using CHROMA (*39*). In addition to the sequences analyzed in Figure 7, we compared the rat CRT with CRT of mouse (Ac. No. O04151), *A. thaliana* (Ac. No. O04151), *C. elegans* (Ac. No. P27798), *D. melanogaster* (Ac. No. P29413), *O. sativa* (Ac. No. Q9SLY8) and CNX from *M. musculus* (Ac. No. P52194) *P. sativum* (Ac. No. O82709), *R. norvegicus* (Ac. No. P35565) and *A. thaliana* (Ac. No. P29402). As observed in Figure 7, the residues corresponding to rat CRT Tyr-109, Met-131, Tyr-128, and Asp-135 were identical in all the sequences. Arg-73 was replaced by Lys in CRT of *C. elegans* and CNX of mouse and rat. Asp317 was replaced by Glu in CRT of mouse, *A. thaliana*, *O. sativa*, and CNX of mouse, pea, rat, and *A. thaliana*. However, Asp at position 125 was not conserved being replaced by a lysine in human and mouse CRT and rat and canine calnexin.

reasons. A trivial explanation is that the interactions made by Asp-125 were not predicted entirely correctly, although our model has proven to be very solid for all other residues. An alternative reason is that the leucine residue could potentially compensate the hydrogen bond energies by having hydrophobic interactions with the sugar. To distinguish between these possibilities, we mutated Asp-125 to both lysine and glycine. If compensatory hydrophobic interactions were the cause of the retained binding, we would expect the glycine mutant to show reduced affinity. On the other hand, as CNX harbors a lysine residue in the corresponding position we would expect D125K mutant to retain the binding affinity observed for the wild-type protein if Asp-125 were to be important for the interaction. However, for neither mutant did we observe any change in the binding affinity for the trisaccharide or tetrasaccharide (Table 2), suggesting that Asp-125 probably does not play any appreciable role in the binding of the sugar to CRT.

Our modeling studies do not show any aromatic residue within the striking distance for stacking with glucose, which could be the reason for the low affinity of glucose to CRT. The importance of stacking interactions between the hydrophobic β-face of the pyranose ring of the monosaccharide for their interactions with the lectins has been demonstrated earlier (*35*). The studies of Sharma and Surolia (*36*) explicitly noted that the failure of *Phaseolus vulgaris* (PHA) lectin to bind to monosaccharides was related to the absence of such a stacking interaction, and indeed the conclusive evidence

was provided by the introduction of an aromatic residue in a PHA mutant that could stack with the monosaccharide which made up for this deficiency of the native protein (*37*). Another example of the importance of stacking interactions is provided by the L127F mutant of *Dolichos biflorus* that again compensates the low affinity of the native protein toward galactose (*38*).

In conclusion, this study pinpoints several CRT residues as being involved in direct interactions with the glycan. Our data provide clear and detailed experimental evidence for the various effects of mutating single CRT residues within the glycan-binding site. In particular, the results underscore the fact that mutations are not tolerated in any of the residues involved in the recognition of the glucose at the nonreducing end. Although contacts occur with the mannoses, interactions involving the glucose residue play a determining role in CRT−saccharide substrate recognition. The result that the 2-deoxy analogue of the disaccharide does not bind to the wild-type CRT further attests to the importance of the presence of glucose at that position in the oligosaccharide substrate.

As mentioned above, many of the residues investigated in CRT, for instance, Tyr-109, Tyr-128, Met-131, and Asp-135, are all strictly conserved in CNX, and Asp-317 is replaced by a Glu. By soaking CNX crystals in glucose, these CNX residues have been observed to form interactions with the glucose (*15*). Thus, we expect that mutation of these residues in CNX will produce similar effects on sugar binding as those described here for CRT. A comparison of the orientation of the Glc_1Man_3 sugar bound in our model of CRT with the glucose bound by CNX is currently not possible, as the coordinates for the complex of CNX and glucose have not been deposited with PDB.

Several studies point to a role of direct protein−protein contacts, in addition to glycan binding, in the interaction between CRT and CNX and their substrates (*12*−*14*). The availability of CRT mutants, such as the Y109F and D135L mutants characterized here, which show no sugar-mediated binding to monoglucosylated substrates, should allow further investigations into the role of protein−protein contacts of CRT and CNX in studies of protein folding in vivo and in vitro.

ACKNOWLEDGMENT

We thank Eva Frickel for help with initial cloning work. The mass spectrometry experiments were conducted at the Molecular Biophysics Unit, mass spectrometry facility funded by the Department of Biotechnology, Government of India, in support of research in the area of proteomics.

REFERENCES

1. Schrag, J. D., Procipio, D. O., Cygler, M., Thomas, D. Y., and Bergeron, J. J. (2003) *Trends Biochem. Sci. 28*, 49−57.
2. Ellgaard, L., Molinari, M., and Helenius, A. (1999) *Science 286*, 1882−1888.
3. Wada, I., Rindress, D., Cameron, P. H., Ou, W.-J., Doherty, J. J., II, Louvard, D., Bell, A. W., Dignard, D., Thomas, D. Y., and Bergeron, J. J. M. (1991) *J. Biol. Chem. 266*, 19599−19610.
4. Ware, F., Vassilakos, A., Peterson, P. A., Jackson, M. R., Lehrman, M. A., and Williams, D. B. (1995) *J. Biol. Chem. 270*, 4697−4704.
5. Hammond, C., Braakman, I., and Helenius, A. (1994) *Proc. Natl. Acad. Sci. U.S.A. 91*, 913−917.
6. Peterson, J. R., Ora, A., Nguyen, Van, P., and Helenius, A. (1995) *Mol. Biol. Cell 6*, 1173−1184.
7. Spiro, R. G., Zhu, Q., Bhoyroo, V., and Söling, H.-D. (1996) *J. Biol. Chem. 271*, 11588−11594.
8. Patil, R. A., Thomas, C. J., and Surolia, A. (2000) *J. Biol. Chem. 275*, 24348−24356.
9. Zapun, A., Darby, N. J., Tessier, D. C., Michalak, M., Bergeron, J. J., and Thomas, D. Y. (1998) *J. Biol. Chem. 273*, 6009−6012.
10. Sousa, M. C., and Parodi, A. J. (1995) *EMBO J. 14*, 4196−4203.
11. Parodi, A. J. (1999) *Biochim. Biophys. Acta 1462*, 287−295.
12. Saito, Y., Ihara, Y., Leach, M. R., Cohen-Doyle, M. F., and Williams, D. B. (1999) *EMBO J. 18*, 6718−6729.
13. Ihara, Y., Cohen-Doyle, M. F., Saito, Y., and Williams, D. B. (1999) *Mol. Cell 4*, 331−341.
14. Stronge, V. S., Saito, Y., Ihara, Y., and Williams, D. B. (2001) *J. Biol. Chem. 276*, 39779−39787.
15. Schrag, J. D., Bergeron, J. J. M., Li, Y., Borisova, S., Hahn, M., Thomas, D. Y., and Cygler, M. (2001) *Mol. Cell 8*, 633−644.
16. Ellgaard, L., Riek, R., Hermann, T., Güntert, P., Braun, D., Helenius, A., and Wüthrich, K. (2001) *Proc. Natl. Acad. Sci. U.S.A. 98*, 3133−3138.
17. Frickel, E.-M., Riek, R., Jelesarov, I., Helenius, A., Wüthrich, K., and Ellgaard, L. (2002) *Proc. Natl. Acad. Sci. U.S.A. 99*, 1954−1959.
18. Leach, M. R., Cohen-Doyle, M. F., Thomas, D. Y., and Williams, D. B. (2002) *J. Biol. Chem. 277*, 29686−29697.
19. Kapoor, M., Srinivas, H., Eaazhisai, K., Gemma, E., Ellgaard, L., Oscarson, S., Helenius, A., and Surolia, A. (2003) *J. Biol. Chem. 278*, 6194−6200.
20. Zahn, R., Buckle, A. M., Perrett, S., Johnson, C. M., Corrales, F. J., Golbik, R., and Fersht, A. R. (1996) *Proc. Natl. Acad. Sci. U.S.A. 93*, 15024−15029.
21. Peterson, J. R., and Helenius, A. (1999) *J. Cell Sci. 112*, 2775−2784.
22. Ho, S. N., Hunt, H. D., Horton, R. M., Pullen, J. K., and Pease, L. R. (1989) *Gene 77*, 51−59.
23. Andrade, M. A., Chacón, P., Merelo, J. J., and Morán, F. (1993) *Protein Eng. 6*, 383−390.
24. Dubois, M., Gilles, K. A., Hamilton, J. K., Rebers, P. A., and Smith, F. (1956) *Anal. Chem. 28*, 350−356.
25. Saha, S. K., and Brewer, C. F. (1994) *Carbohydr. Res. 254*, 157−167.
26. Oscarson, S., and Tedebark, U. (1995) *Carbohydr. Res. 278*, 271−287.
27. Wiseman, T., Williston, S., Brandts, J. F., and Lin, L. N. (1989) *Anal. Biochem. 179*, 131−137.
28. Yang, C. P. (1990) Omega Data in Origin, p 66, Microcal Inc., Northampton, MA.
29. Srinivas, V. R., Bhanuprakash Reddy, G., and Surolia, A. (1999) *FEBS Lett. 450*, 181−185.
30. Fersht, A. R., Shi, J. P., Knill-Jones, J., Lowe, D. M., Wilson, A. J., Blow, D. M., Brick, P., Corles, P., Waye, M. M. Y., and Winter, G. (1985) *Nature 314*, 235−238.
31. Sharma, V., and Surolia, A. (1997) *J. Mol. Biol. 267*, 433−445.
32. Baksh, S., and Michalak, M. (1991) *J. Biol. Chem. 266*, 21458−21465.
33. Bouvier, M., and Stafford, W. (2000) *Biochemistry 39*, 14950−14959.
34. Li, Z., Stafford, W. F., and Bouvier, M. (2001) *Biochemistry 40*, 11193−11201.
35. Chandra, N. R., Prabu, M. M., Suguna, K. and Vijayan, M. (2001) *Protein Eng. 14*, 857−866.
36. Sharma, V., and Surolia, A. (1997) *J. Mol. Biol. 267*, 433−445.
37. Hamelryck, T. W., Dao-Thi, M. H., Poortmans, F., Chrispeels, M. J., Wyns, L. and Loris, R. (1996) *J. Biol. Chem. 271*, 20479−20485.
38. Hamelryck, T. W., Loris, R., Bouckaert, J., Dao-Thi, M. H., Strecker, G., Imberty, A., Fernandez, E., Wyns, L., and Etzler, M. E. (1999) *J. Mol. Biol. 286*, 1161−77.
39. Goodstadt, L., and Ponting, C. P. (2001) *Bioinformatics 17*, 845−846.

BI0355286